J Mater Sci (2011) 46:7198–7205
DOI 10.1007/s10853-010-4638-6

Use of single wall carbon nanohorns in polymeric electrolyte fuel cells

Lúcia Brandão · Carolina Passeira · Daniele Mirabile Gattia · Adélio Mendes

Received: 13 November 2009 / Accepted: 21 May 2010 / Published online: 5 June 2010

Abstract Single wall carbon nanohorns (SWNH), produced by AC arc discharge in air, were used as Pt and PtRu supports in polymer electrolyte membrane fuel cells (PEMFC). These electrocatalysts were compared with equivalent electrocatalysts supported on commercial carbon back. The SWNH were characterized by differential thermal analysis (DTA), TEM, SEM, and XRD. The produced SWNH were 84.5 wt% pure, containing 3 wt% of amorphous carbon and 12.5 wt% of graphitic carbon. SWNH were used as electrocatalyst supports and tested in the electrodes of two types of polymer electrolyte fuel cells: H_2-fed PEMFC and direct methanol fuel cells (DMFC). The electrocatalyst nanoparticles anchored on both carbon supports were ca. 2.5 nm in diameter obtained by employing ethylene glycol as the reducing agent. The use of SWNH showed catalytic activities 60% higher than using carbon black as the electrocatalyst support in both types of fuel cells.

This paper follows from a presentation at Hyceltec 2009, the 2nd Iberian Symposium on Hydrogen, Fuel Cells and Advanced Batteries. Guest Editor: Verónica Cortés de Zea Bermudez.

L. Brandão (✉) · C. Passeira · A. Mendes
Laboratório de Engenharia de Processos, Ambiente e Energia (LEPAE), Faculdade de Engenharia do Porto, Rua Roberto Frias, 4200-465 Porto, Portugal
e-mail: lbrandao@fe.up.pt

D. Mirabile Gattia
MAT-COMP, ENEA, Via Anguillarese 301, 00123 Rome, Italy

Introduction

The electrocatalyst support used in the electrodes of polymer electrolyte membrane fuel cells (PEMFC) is very important because carbon support can greatly affect the electrochemical activity obtained. Owing to that, different forms of carbon structures alternative to the commonly used carbon black have been suggested and have been recently summarized by Antolini [1]. The desired main features of these new carbon structures are a high surface area and a good crystallinity that can provide both high dispersion of electrocatalyst nanoparticles and facilitate electron transfer; a suitable porosity allowing good reactants fluxes is also very important. Among possible carbon structures, carbon nanotubes [2, 3], carbon nanohorns [4–6], and graphene [7] have been suggested and showed interesting performances when compared with carbon black.

Single wall carbon nanohorns (SWNH) have a similar graphene structure as carbon nanotubes displaying, however, a horn-shaped tip at the top of the single wall nanotube instead of the half fullerene cap observed in nanotubes. They are ca. 2–10 nm in diameter and 10–70 nm in length [8] and self-assemble in aggregates of about 20–100 nm [6]. SWNH display a great variety of particle aggregates being the most common the so-called bud-like or dahlia-like, according the horn tip is inside the aggregate particle or protruding the aggregate particle [9, 10]. SWNH have been usually produced by arc discharge and CO_2 laser ablation, both starting from graphite. The state of the art laser ablation devices for producing SWNH use a three-chamber system and can produce up to 60 g h^{-1}, two decades above the productivity of simpler devices [10]. In its turn, production rates by arc discharge are presently lower (18 g h^{-1}). However, arc discharge is a

preferable method because it is cheaper [11]. Moreover, current investigation using arc discharge is still going on in order to increase productivity and decrease production costs by using less pure graphite electrodes [12]; these developments will result ultimately in a wider use of SWNH [13, 14].

Single wall carbon nanohorns have been characterized by Raman spectroscopy and X-ray Photoelectron Spectroscopy (XPS) in order to infer its assembly structure. It was observed that SWNH particles aggregate through not only van der Waals forces but also by chemical bonding [15]; very recently, however, it was succeeded the individual isolation of SWNH by density gradient centrifugation [8]. SWNH have been deeply characterized in terms of surface area and porosity [16, 17] due to its promising properties for gas adsorption, additionally they were modified by oxidation in order to increase its surface area up to ca. 1000 $m^2\ g^{-1}$ [18, 19]. Finally, differential thermal analysis (DTA) has been largely used to characterize SWNH purity where most common impurities are amorphous carbon and giant graphitic balls [18, 20, 21].

Single wall carbon nanohorns have been applied in the fields of nanomedicine mainly for cancer therapy [22–24], gas sensors [25–27], biosensors [28–30], drug delivery and carrier systems [13, 24, 31–33], in hydrogen storage systems [34], and as counter electrode in dye-sensitized solar cells [35].

Additionally, the use of SWNH can also be very promising in fuel cells not only because of its high surface area, but also because of its high electrical conductivity that results from the close contact among the SWNH in the aggregates. Additionally, the self-assembling nature of the aggregates allows reactants to easily diffuse to make contact with the catalyst. SWNH have been previously suggested for fuel cell electrodes in few patents [14, 36]; however, their potential when used as electrocatalyst support needed to be further addressed. For instance, it was observed an increase of ca. 50% in the PEMFC performance when carbon black was replaced by SWNH to support the electrocatalysts [37]. A direct correlation between SWNH surface area and PEMFC performance was observed [4]. In its turn, a very high improvement in passive direct methanol fuel cells (DMFC) performances was observed by using SWNH to support the Pt catalyst [38]. Despite these studies, the direct comparison between the performance of a DMFC employing a catalyst supported on SWNH and on carbon black has never been studied.

In this study, SWNH aggregates were synthesized by AC arc discharge in air and characterized. Following, SWNH were used as electrocatalyst support in the electrodes of DMFC and PEMFC and the performance compared with corresponding electrocatalysts supported on commercial carbon black.

Experimental section

SWNH synthesis

The synthesis of SWNH was performed by using AC arc discharge in air [9]. The arc discharge was ignited between two pure graphite electrodes approaching each other at a constant speed of 4 mm min^{-1}, and was powered by an AC generator at a frequency of 35 Hz at 28 V and 90 A [5].

Electrocatalysts deposition

Ethylene glycol (EG) was used as reducing agent in order to anchor Pt and Pt/Ru (1:1 atomic ratio) nanoparticles on the carbon supports [5]. Briefly, SWNH or carbon black (Vulcan XC-72R, Cabot) was previously suspended in an EG solution (5 vol% of water in EG), and the required amount of a 0.8 wt% metal catalyst solution ($H_2PtCl_6 \cdot 6H_2O$ and $RuCl_3$, both from Sigma-Aldrich) in the EG solution was added drop wise. NaOH was added to adjust pH above 13, and the mixture was refluxed for 3 h. The sample was filtered and dried for 8 h at 80 °C.

Characterization

The microstructure and morphology of the different materials were characterized by transmission electron microscopy (TEM) and by field emission scanning electron microscopy (FE-SEM) equipped with an Energy Dispersive X-ray Spectroscopy (EDS) detector. The samples analyzed by TEM were prepared by dropping a small amount of electrocatalyst suspension, dispersed in ethanol by ultrasounds, on a thin copper grid holder covered by a conductive layer of amorphous carbon. In its turn, for SEM analysis, a small amount of electrocatalyst suspension was dropped on graphite covered aluminum stubs.

The crystallite size of the electrocatalysts and the crystalline pattern of the carbon supports were evaluated by X-ray diffraction (XRD), with a Cu Kα source radiation. The $20° \leq 2\theta \leq 85°$ range was studied with a scan step size of 0.02° and a fixed counting time of 1s, while the (220) reflection of Pt (62–72° 2θ) was studied with a scan step size of 0.02° and a scan step time of 3 s.

Differential thermal analysis (DTA/TG) was used to evaluate SWNH purity using a heating rate of 3 °C min^{-1} up to 1000 °C with an air flow of 100 mL min^{-1}. Thermogravimetric analysis (TGA) was used to evaluate the metal content of the electrocatalyst powder. It was used an oxygen input flow rate of 30 mL min^{-1} and a heating rate of 10 °C min^{-1} up to 900 °C. N_2 adsorption isotherm at 77 K was used to evaluate the BET surface area of the carbon supports.

Pt and Pt Ru nanoparticles supported on both SWNH and carbon black were analyzed by XPS. Powder samples needed to be supported in a carbon tape. XPS core-level spectra were obtained using a spectrometer system equipped with a polychromatic Mg Kα X-ray source at 15 kV.

Electrodes preparation

Gas diffusion layer (GDL) of the DMFC electrodes were in-house assembled using carbon cloth covered with 4 mg cm^{-2} of a microporous carbon black layer mixed with 15 wt% Teflon with respect to the carbon black [5]. Regarding the PEMFC electrodes, they were used Sygracet commercial GDLs, hydrophobized with 5 wt% of PTFE and covered with a proprietary microporous layer (SGL Carbon, ref.: GDL 24 BC).

The catalytic layers were spray dried on the GDL microporous surface followed by drying at room temperature overnight [5]. Briefly, a homogeneous suspension of the catalyst powder was prepared with isopropyl alcohol and 20 wt% Nafion with respect to the supported catalyst. The catalyst load was obtained based on the difference between the weights of the microporous GDL before and after the spray drying (Table 1).

Fuel cell tests

The DMFC and PEMFC runs were carried out in a 5-cm^2 single cell hardware and with a 4 cm^2 electrodes area. For the DMFC performance experiments, it was used a 117-Nafion membrane as polymer electrolyte [5]. Tests were performed at 50 °C by feeding a 2 M methanol solution to the anode side at 2 mL min^{-1} and by feeding the cathode side with 200 mL_N min^{-1} oxygen at atmospheric pressure and 30% relative humidity.

In its turn, the PEMFC runs were performed using a 1135-Nafion membrane at 50 °C. The cell was fed with 500 mL min^{-1} of hydrogen and 500 mL min^{-1} of synthetic air, both streams with 80% relative humidity and 2 bar. In both cases, polarization curves were obtained in triplicate.

Table 1 BET surface area, electrocatalyst content on the supports tested, and the electrocatalyst load on the different electrodes prepared

Support	Carbon black	SWNH
BET surface area (m^2 g^{-1})	231	176
DMFC PtRu content on support (wt%)	12	12
DMFC Pt content on support (wt%)	10	10
PEMFC Pt content on support (wt%)	18	16
DMFC anode load (mg_{PtRu} cm^{-2})	0.9	0.9
DMFC cathode load (mg_{Pt} cm^{-2})	0.5	0.5
PEMFC electrodes load (mg_{Pt} cm^{-2})	0.6	0.3

Results and discussion

SWNH synthesis and characterization

Single wall carbon nanohorns were synthesized by AC arc discharge in air [9, 39] at 35 Hz and 28 V. At these conditions (low frequency and high voltage), it was obtained the highest yield of high purity SWNH (ca. 16 g h^{-1}) [39]. Figure 1a shows an SEM micrograph of the synthesized SWNH particles, where aggregates show the so-called dahlia-like structure [9, 10]. In such aggregate, the tips of the SWNH are protruding from the aggregate and a rough surface is observed. Figure 1b shows a TEM image of the dahlia-like SWNH exhibiting the conic tips protruding from the aggregate particle in greater detail. Figure 1c shows the so-called bud-like aggregate [9, 10], where the conic tips of the nanohorns are inside the aggregate making the aggregate surface less rough. From TEM and SEM observations, it could be inferred that the main SWNH aggregate type present in the sample is the bud-like structure together with very few graphitic giant balls [9, 39].

In order to infer their purity, synthesized SWNH were characterized by DTA [10, 18]. Figure 2 shows the exothermic heat flow and weight loss as a function of the burning temperature. A first small and broad peak at nearly 350 °C can be observed in the DTA plot. This is related to the burning of the amorphous carbon present in the sample [18]. At this temperature ca. 3 wt% of the sample was burned out corresponding to amorphous carbon impurities. In the temperature range between 400 °C and nearly 600 °C SWNH are burned out [10, 18]. On the other hand, at temperatures higher than 600 °C graphitic impurities corresponding to the graphitic giant balls are burned out [21], corresponding to ca. 12.5 wt% of the SWNH sample. According to these results, the composition of the SWNH sample is approximately: 3 wt% amorphous carbon, 84.5 wt% SWNH, and 12.5 wt% graphitic carbon. This purity level is comparable to values reported in other studies [4, 18, 40].

Regarding the SWNH burning between 400 °C and 600 °C, at lower temperatures ($T < 500$ °C) occurs the burning out of the horn tip composed mainly by the defective 5-carbon rings. Once 5-carbon rings are not stable as tubular graphene, the tips are burned out easier [18]. The peak related to the horn tip burning out is very broad, and it is overlapped by the beginning of the tubular graphene burning at ca. 500 °C, as reported previously [18].

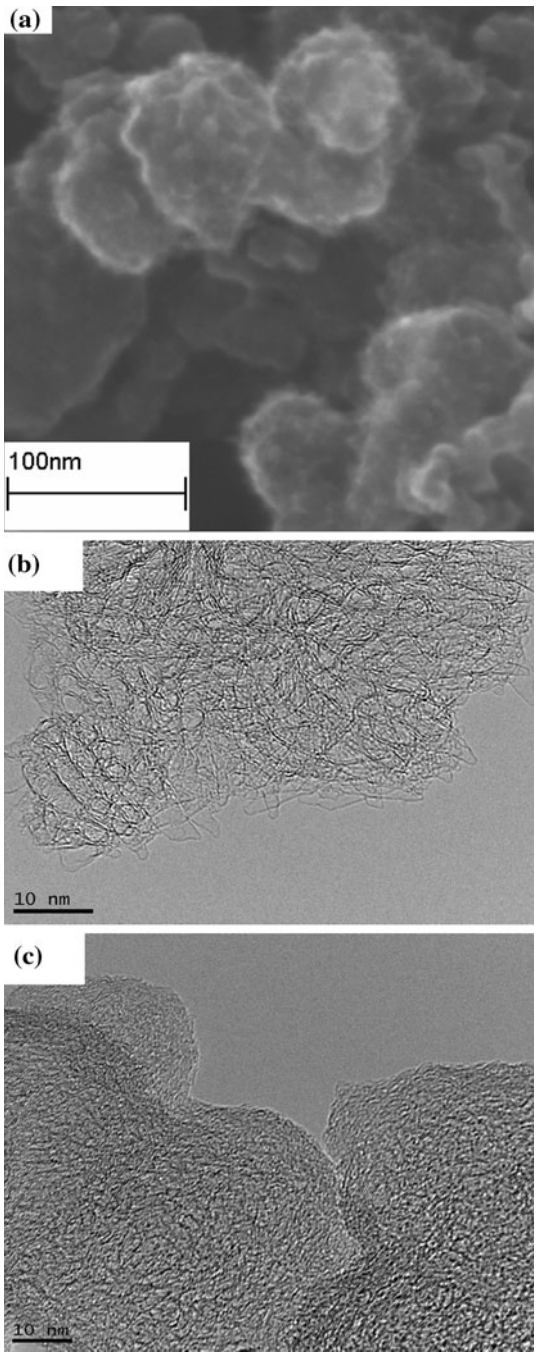

Fig. 1 Micrographs of the synthesized SWNH: **a** SEM, **b** TEM image of the dahlia-like aggregate, **c** TEM image of the bud-like aggregate

Electrocatalyst characterization

Pt and Pt/Ru electrocatalysts were supported on commercial carbon black and SWNH in order to compare the performance of both supports in DMFC and PEMFC applications. The metal electrocatalysts were deposited in both carbon structures from a metal salt solution and using ethylene glycol as reducing agent. Electrocatalyst particle size and its distribution on the carbon supports were characterized by XRD, TEM, and SEM; electrocatalyst content was determined by TGA.

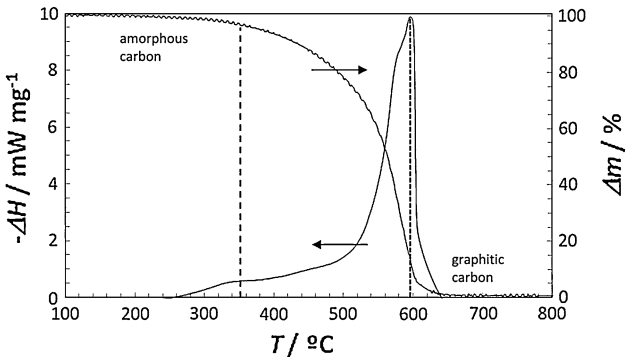

Fig. 2 DTA and weight loss as function of temperature for the synthesized SWNH sample

Figure 3 shows the XRD pattern of Pt electrocatalyst on carbon black and SWNH supports. The diffraction peaks of the carbon supports related to the hexagonal graphite structure appear at 25.5° (002) and 42.4° (100). A wider (002) peak is observed corresponding to carbon black pattern, which is characteristic of amorphous carbon with only small regions of crystallinity. On the other hand, SWNH sample shows a broad (002) peak constituted by two main components: the broader component at lower angles due to diffraction of two graphene planes one near the other (the walls of SWNH tubes), as reported by Bandow and co-workers [41], and a straight and sharp (002) peak at higher angles due to the presence of the graphitic carbon, as just stated above. The typical diffraction peaks of Pt are around 39.7° (111) and 67.8° (220) and can be observed in the diffractogram for both carbon support samples. The average Pt crystallite size was obtained from the Scherrer's equation at Pt (220) diffraction peak, because there is not overlapping with reflections due to other phases. The mean electrocatalyst particle diameter is approximately 3 nm for both carbon supports, indicating the very small particle size that can be obtained

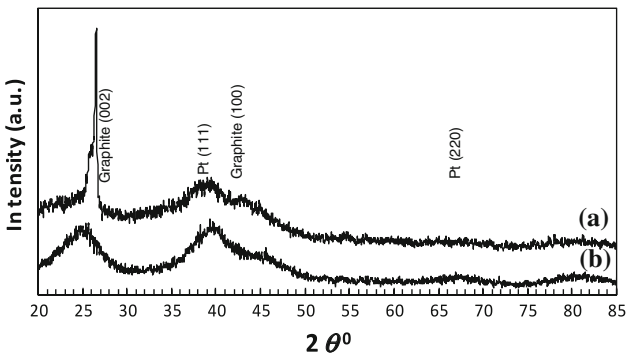

Fig. 3 Powder XRD pattern of Pt/SWNH (**a**) and Pt/C (**b**) catalysts

by using the ethylene glycol reduction method, in accordance with other works using the same method [3].

Figures 4 and 5 show the metallic nanoparticles deposited on carbon black and SWNH observed by SEM and TEM. Figure 4a and b shows the Pt and PtRu electrocatalysts, respectively, observed by SEM on the carbon black support. These images show that the metal nanoparticles

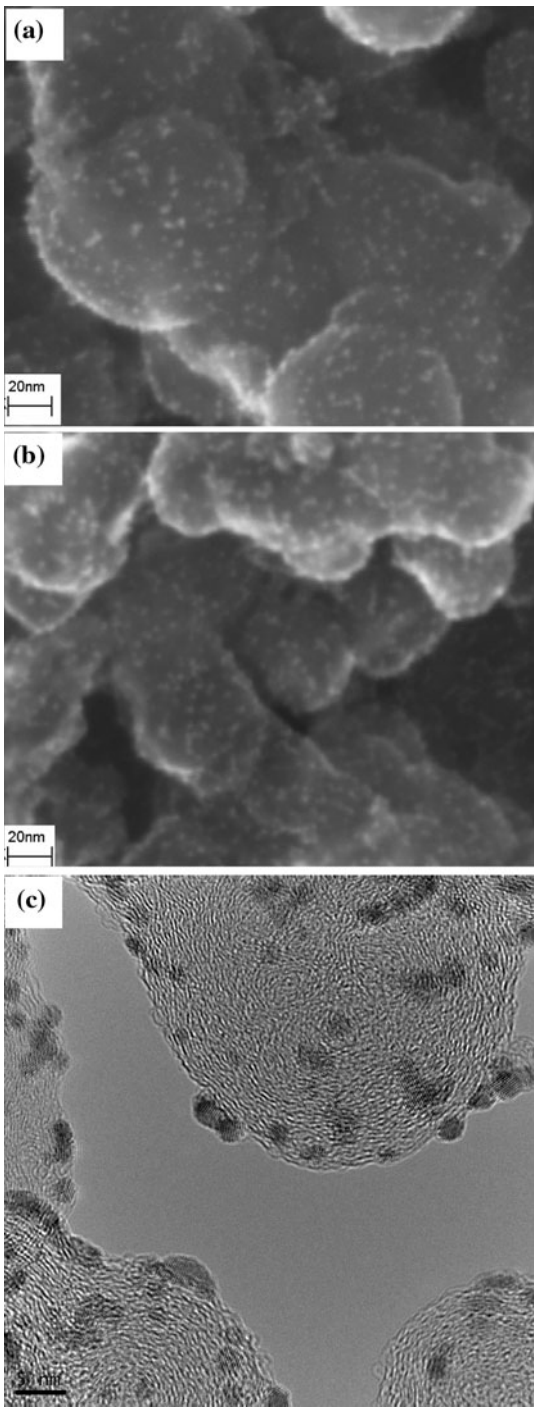

Fig. 4 Micrographs of Pt and Pt/Ru nanoparticles deposited on carbon black (Vulcan XC-72R): **a** SEM, Pt, **b** SEM, PtRu, **c** TEM, Pt

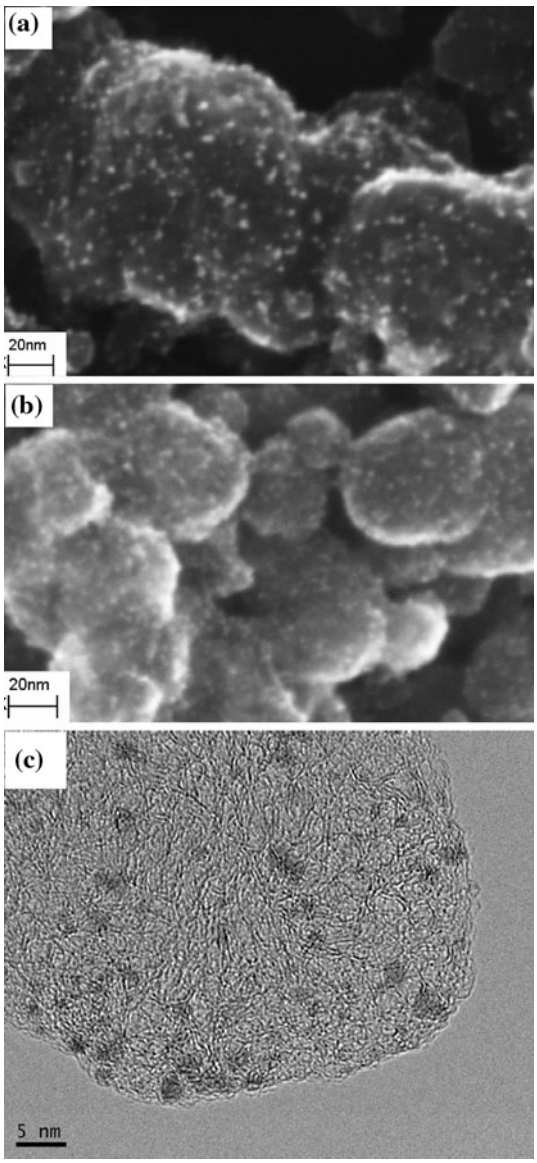

Fig. 5 Micrographs of Pt and Pt/Ru nanoparticles deposited on SWNH: **a** SEM, Pt, **b** SEM, PtRu, **c** TEM, Pt

are uniformly distributed on the carbon black surface. SEM/EDS confirmed the atomic ratio 1:1 in both Pt:Ru samples. Figure 4c shows a TEM image of the Pt nanoparticles supported on carbon black. The average Pt particle diameter observed is ca. 2.5 nm, in accordance with XRD results. Figure 5a and b shows the metallic nanoparticles of Pt and PtRu, respectively, supported on the synthesized SWNH. The metallic dispersion is also high and very similar to the one observed on the carbon black (Fig. 4). Figure 5c shows the TEM micrograph of the Pt electrocatalyst deposited on the SWNH where a small Pt particle size, ca. 2.5 nm in average, can also be observed.

The XPS spectra for Pt(4f) and Ru(3d) core levels of the Pt and PtRu electrocatalysts supported on carbon black and

SWNH are shown in Fig. 6. The Pt(4f) and Ru (3d) regions exhibit doublets from the spin–orbit splitting of the 4f5/2 and 4f7/2 and 3d3/2 and 3d5/2 states. The XPS spectra for the Ru (3d) core level is slightly overlayered with the C(1s) XPS peak; however, deconvolution results indicate that Ru present in the PtRu samples is in metallic state (Fig. 6c, f). In its turn, the XPS spectra suggest the presence of two or three chemically different Pt states (Fig. 6a, b, d and e). In these figures, the major peak is due to metallic Pt (in the range from 71.8 to 72.5 eV), and the other peaks are attributed to oxidized species. The carbon black (Fig. 6a–c) and SWNH (Fig. 6d–f) supported electrocatalysts showed essentially identical ratio of metallic Pt to oxide species (ca. 75% in average). The slight shift observed for the Pt(4f7) peaks (71.2 eV) toward higher binding energies in all the samples is a known effect for small particles [42].

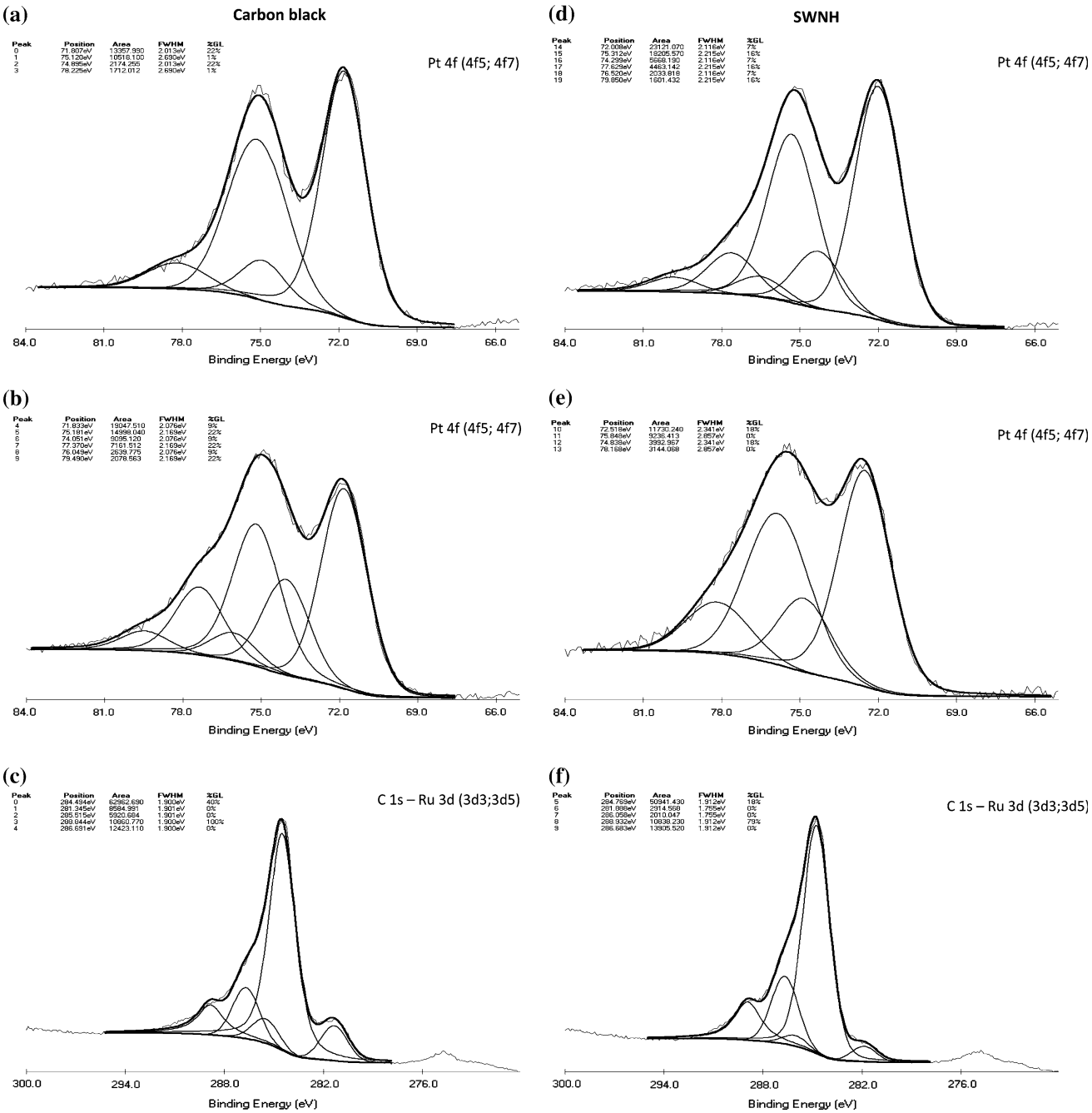

Fig. 6 XPS spectra of the different electrocatalysts. Carbon black supported: **a** Pt (Pt4f); **b** PtRu (Pt4f); **c** PtRu (C1s; Ru3d); SWNH supported; **d** Pt (Pt4f); **e** PtRu (Pt4f); **f** PtRu (C1s; Ru3d)

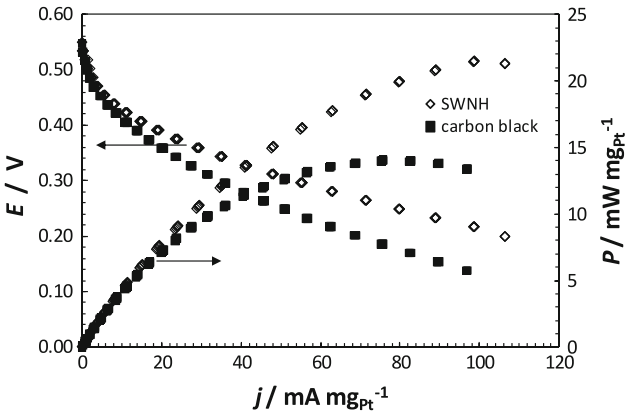

Fig. 7 Comparison of DMFC performances of the MEAs tested with different carbon supports at 50 °C

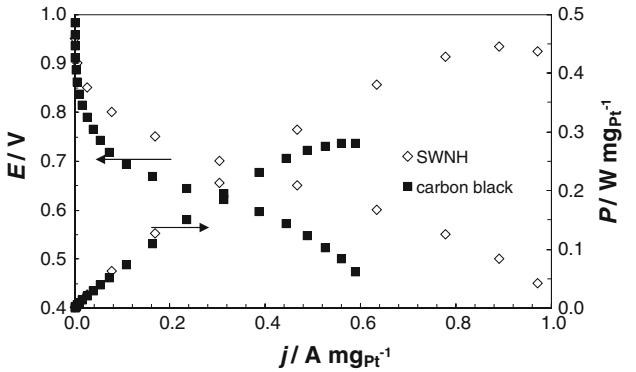

Fig. 8 Comparison of PEMFC performances of the MEAs tested with different carbon supports at 50 °C

The metallic Pt:Ru atomic ratio calculated from the XPS analysis confirmed the proportion of 1:1 for the PtRu supported carbon black electrocatalyst, in accordance with SEM/EDS analyses. It was observed a slightly higher proportion of Pt (1.5:1) in the PtRu supported SWNH sample.

It may be concluded that the metal catalysts exhibit in both supports approximately the same morphology, beyond having approximately the same load, Table 1. This enables us to compare the influence of the catalysts support on the DMFC and PEMFC performance.

Fuel cell tests

The prepared supported catalysts were used to make the electrodes for the PEMFC and DMFC tests. Figures 7 and 8 show the polarization curves obtained for both samples tested under the same operating conditions. Table 1 shows the electrocatalyst load in each of the electrodes prepared, the electrocatalyst content in the carbon supports, and the BET surface area of both the carbon supports. Surface area of the SWNH sample (176 m^2 g^{-1}) is in agreement with some references [4] while lower than other works (ca. 300 m^2 g^{-1} [43, 44]). The larger surface area observed for the carbon black sample is related to the presence of more micropores (data not shown) in comparison to SWNH [1]. Actually, carbon black has a micropore surface area fraction ca. 30% higher than SWNH, indicating that SWNH structure is more open than the carbon black one.

Figure 7 shows the DMFC performance for both the carbon supports. It is clear that SWNH support shows a better performance in comparison with the carbon black support; the peak power density of the DMFC with SWNH increased 60% compared with the one with carbon black.

Figure 8 shows the PEMFC performance obtained also with the two types of catalyst carbon supports. Once more, SWNH showed ca. 60% increase in peak power density compared with carbon black. This is in accordance with previous results that showed 50% increase in PEMFC performance of SWNH support compared with the one with carbon black [14]. In both DMFC and PEMFC runs, electrochemical impedance spectroscopy (EIS) indicated similar proton conductivities of the membranes within each fuel cell technology.

These results show that the use of SWNH for supporting fuel cell electrocatalysts is very promising. In this study, the electrocatalyst content obtained on both carbon supports and the BET surface areas was similar (Table 1) and both support types have the same electrocatalyst particle size with a uniform distribution. This way, the better performance of SWNH should be related to the high electrical conductivity and the more open structure of the SWNH aggregates. Future work is undergoing in order to understand the increased performance obtained in fuel cells.

Conclusions

Single wall carbon nanohorns were synthesized by AC arc discharge in air at a low frequency (35 Hz). The SWNH sample prepared is composed by 84.5 wt% SWNH aggregates, 3 wt% amorphous carbon, and 12.5 wt% graphitic carbon. The SWNH were used to support electrocatalyst nanoparticles of Pt and PtRu with ca. 2.5 nm in diameter, using ethylene glycol as the reducing agent of the precursor metal salts. The performance of electrocatalysts supported on both commercial carbon black and SWNH was evaluated when inserted on a PEMFC and a DMFC. The SWNH support exhibits in both cases peak power densities 60% higher than when using carbon black as catalyst support. It was then concluded that the use of SWNH is very promising as electrocatalyst support.

Acknowledgements Lúcia Brandão is grateful to the Portuguese Foundation for Science and Technology (FCT) for her post-doc grant (reference SFRH/BPD/41233/2007). Financial support by FCT through the project PTDC/EQU-EQU/70574/2006 is also acknowledged.

References

1. Antolini E (2009) Appl Catal B 88:1
2. Ocampo AL, Miranda-Hernandez M, Morgado J, Montoya JA, Sebastian PJ (2006) J Power Sources 160:915
3. Li WZ, Wang X, Chen ZW, Waje M, Yan YS (2006) J Phys Chem B 110:15353
4. Sano N, Kimura Y, Suzuki T (2008) J Mater Chem 18:1555
5. Brandão L, Mirabile Gattia D, Marazzi R, Vittori Antisari M, Licoccia S, Epifanio A, Traversa E, Mendes A (2010) Mater Sci Forum 638–642:1106
6. Mirabile Gattia D, Vittori Antisari M, Giorgi L, Marazzi R, Piscopiello E, Montone A, Bellitto S, Licoccia S, Traversa E (2009) J Power Sources 194:243
7. Yoo E, Okata T, Akita T, Kohyama M, Nakamura J, Honma I (2009) Nano Lett 9:2255
8. Zhang MF, Yamaguchi T, Iijima S, Yudasaka M (2009) J Phys Chem C 113:11184
9. Mirabile Gattia D, Vittori Antisari M, Marazzi R (2007) Nanotechnology 18:7
10. Azami T, Kasuya D, Yuge R, Yudasaka M, Iijima S, Yoshitake T, Kubo Y (2008) J Phys Chem C 112:1330
11. Wang H, Chhowalla M, Sano N, Jia S, Amaratunga GAJ (2004) Nanotechnology 15:546
12. Sano N, Yasumura Y, Kimura Y, Toyoda A, Hirano K (2008) Trans Mat Res Soc Jap 33:669
13. Iijima S, Yudasaka M, Komi F, Takahashi K, James Adelene N (2005) Material for adsorbing gases, organic material, complex and bio related substance, comprises mono layer carbon nanohorn aggregate formed by aggregating mono layer carbon nanohorns in ball shape, JP2005021892-A
14. Kurungot S, Kurungott S (2007) Electrode catalyst for a solid polymer fuel cell, comprises a carbon nanohorn aggregate as a support, a catalytic metal supported on the carbon nanohorn aggregate support, and a polyelectrolyte applied to the aggregate support, WO2007105576-A2
15. Utsumi S, Honda H, Hattori Y, Kanoh H, Takahashi K, Sakai H, Abe M, Yudasaka M, Iijima S, Kaneko K (2007) J Phys Chem C 111:5572
16. Urita K, Seki S, Utsumi S, Noguchi D, Kanoh H, Tanaka H, Hattori Y, Ochiai Y, Aoki N, Yudasaka M, Iijima S, Kaneko K (2006) Nano Lett 6:1325
17. Yuge R, Ichihashi T, Miyawaki J, Yoshitake T, Iijima S, Yudasaka M (2009) J Phys Chem C 113:2741
18. Utsumi S, Miyawaki J, Tanaka H, Hattori Y, Itoi T, Ichikuni N, Kanoh H, Yudasaka M, Iijima S, Kaneko K (2005) J Phys Chem B 109:14319
19. Fan J, Yudasaka M, Miyawaki J, Ajima K, Murata K, Iijima S (2006) J Phys Chem B 110:1587
20. Fan J, Yudasaka M, Kasuya D, Azami T, Yuge R, Imai H, Kubo Y, Iijima S (2005) J Phys Chem B 109:10756
21. Azami T, Kasuya D, Yoshitake T, Kubo Y, Yudasaka M, Ichihashi T, Iijima S (2007) Carbon 45:1364
22. Whitney J, Sarkar S, Zhang JF, Shu CY, Dorn H, Rylander C, Campbell T, Geohegan D, Rylander MN (2009) In: 29th annual conference of the American-Society-for-Laser-Medicine and Surgery. Lasers in Surgery and Medicine, National Harbor, MD, p 3-3
23. Zhang M, Murakami T, Ajima K, Tsuchida K, Sandanayaka ASD, Ito O, Iijima S, Yudasaka M (2008) Proc Natl Acad Sci USA 105:14773
24. Murakami T, Sawada H, Tamura G, Yudasaka M, Iijima S, Tsucbida K (2008) Nanomed 3:453
25. Sano N, Ohtsuki F (2007) J Electrostat 65:263
26. Sano N, Kinugasa M, Otsuki F, Suehiro J (2007) Adv Powder Tech 18:455
27. Suehiro J, Sano N, Zhou GB, Imakiire H, Imasaka K, Hara M (2006) J Electrostat 64:408
28. Shi LH, Liu XQ, Niu WX, Li HJ, Han S, Chen J, Xu GB (2009) Biosens Bioelect 24:1159
29. Sandanayaka ASD, Ito O, Zhang MF, Ajima K, Iijima S, Yudasaka M, Murakami T, Tsuchida K (2009) Adv Mat 21:4366
30. Liu XQ, Shi LH, Niu WX, Li HJ, Xu GB (2008) Biosens Bioelectron 23:1887
31. Battiston S, Bolzan M, Fiameni S, Gerbasi R, Meneghetti M, Miorin E, Mortalo C, Pagura C (2009) Carbon 47:1321
32. Lacotte S, Garcia A, Decossas M, Al-Jamal WT, Li S, Kostarelos K, Muller S, Prato M, Dumortier H, Bianco A (2008) Adv Mat 20:2421
33. Ajima K, Murakami T, Mizoguchi Y, Tsuchida K, Ichihashi T, Iijima S, Yudasaka M (2008) ACS Nano 2:2057
34. Sahaym U, Norton MG (2008) J Mater Sci 43:5395. doi:10.1007/s10853-008-2749-0
35. Huang Z, Liu XH, Li KX, Li DM, Luo YH, Li H, Song WB, Chen LQ, Meng QB (2007) Electrochem Commun 9:596
36. Kosaka M, Kuroshima S, Yudasaka M, Yuge R (2009) Processing of carbon-nanohorn aggregate used for fuel-cell catalysts, involves opening hole which does not allow substance with diameter more than preset value to pass through, by heating aggregate in hydrogen-peroxide solution, JP2009190928-A
37. Yoshitake T, Shimakawa Y, Kuroshima S, Kimura H, Ichihashi T, Kubo Y, Kasuya D, Takahashi K, Kokai F, Yudasaka M, Iijima S (2002) Physica B 323:124
38. Kosaka M, Kuroshima S, Kobayashi K, Sekino S, Ichihashi T, Nakamura S, Yoshitake T, Kubo Y (2009) J Phys Chem C 113:8660
39. Mirabile Gattia D, Vittori Antisari M, Marazzi R, Piscopiello E, Montone A (2008) In: Bandaru PR, Grego S, Kinloch I (eds) Symposium on nanotubes, nanowires, nanobelts and nanocoils held at the 2008 MRS fall meeting. Boston, MA, pp 49–54
40. Kasuya D, Yudasaka M, Takahashi K, Kokai F, Iijima S (2002) J Phys Chem B 106:4947
41. Bandow S, Kokai F, Takahashi K, Yudasaka M, Qin LC, Iijima S (2000) Chem Phys Lett 321:514
42. Garbarino S, Pereira A, Hamel C, Irissou E, Chaker M, Guay D (2010) J Phys Chem C 114:2980
43. Murata K, Kaneko K, Kokai F, Takahashi K, Yudasaka M, Iijima S (2000) Chem Phys Lett 331:14
44. Bekyarova E, Kaneko K, Yudasaka M, Kasuya D, Iijima S, Huidobro A, Rodriguez-Reinoso F (2003) J Phys Chem B 107:4479